

Comparison of Four Cloud Schemes in Simulating the Seasonal Mean Field Forced by the Observed Sea Surface Temperature

AKIHIKO SHIMPO,* MASAO KANAMITSU, AND SAM F. IACOBELLIS

Scripps Institution of Oceanography, University of California, San Diego, La Jolla, California

SONG-YOU HONG

Global Environment Laboratory, Department of Atmospheric Sciences, Yonsei University, Seoul, South Korea

(Manuscript received 20 February 2007, in final form 10 October 2007)

ABSTRACT

The impacts of four stratiform cloud parameterizations on seasonal mean fields are investigated using the global version of the Experimental Climate Prediction Center (ECPC) global-to-regional forecast system (G-RSM). The simulated fields are compared with the International Satellite Cloud Climatology Project (ISCCP) data for clouds, the Global Precipitation Climatology Project data for precipitation, the Earth Radiation Budget Experiment and the Surface Radiation Budget data for radiation, and the National Centers for Environmental Prediction (NCEP)–Department of Energy (DOE) Atmospheric Model Inter-comparison Project (AMIP-II) Reanalysis (R-2) for temperature.

Compared to observations, no stratiform cloud parameterization performed better in simulating all aspects of clouds, temperature, precipitation, and radiation fluxes. There are strong interactions between parameterized stratiform clouds and boundary layer clouds and convection, resulting in changes in low-level cloudiness and precipitation in the simulations.

When the simulations are compared with ISCCP cloudiness and cloud water, and the NCEP/DOE R-2 relative humidity, the cloud amounts simulated by all four cloud schemes depend mostly on relative humidity with less dependency on the model's cloud water, while the observed cloud amount is more strongly dependent on cloud water than relative humidity, suggesting that cloud parameterizations and the simulation of cloud water require further improvement.

1. Introduction

Clouds are one of the most uncertain components in climate models and model results are known to be very sensitive to their parameterization. Accurate simulations of cloud amount, vertical distribution, and the radiative property of clouds are particularly important for ocean–atmosphere coupling because of the large impact of clouds on short- and longwave radiation fluxes reaching the ocean.

To improve the simulation of cloud amount,¹ several cloudiness parameterizations have been proposed (e.g., Stephens 2005), which can be divided into the following three types. The first is based on the probability density function (PDF) of the subgrid-scale distributions of the cloud water and cloud amount (e.g., Smith 1990; Lohmann et al. 1999; Rotstayn et al. 2000; Tompkins 2002). In the second type, cloud amount is diagnosed from

* On leave from the Climate Prediction Division, Japan Meteorological Agency, Tokyo, Japan.

Corresponding author address: Akihiko Shimpo, Climate Prediction Division, Japan Meteorological Agency, 1-3-4 Ote-machi, Chiyoda-Ku, Tokyo 100-8122, Japan.
E-mail: ashimpo@naps.kishou.go.jp

¹ In numerical weather prediction (NWP) models and general circulation models (GCMs), the portion of precipitation from a microphysical process and its precipitation processes is regarded as grid-resolvable precipitation, and the parameterized processes from the cumulus parameterization scheme is regarded as sub-grid-scale precipitation. In this study, the cloudiness and precipitation from the grid-resolvable precipitation algorithm are defined by stratiform clouds and large-scale precipitation, whereas they are termed as convective clouds and convective precipitation for the cumulus parameterization scheme.

relative humidity (e.g., Slingo 1987; Slingo and Slingo 1991) or from both relative humidity and cloud water (e.g., Randall 1995; Xu and Randall 1996). In the third type, cloud amount is predicted as a prediction variable using an equation considering the sources and sinks of cloud amount (e.g., Tiedtke 1993). There are other types of cloud parameterizations, particularly for convective (Bony and Emanuel 2001) and boundary layer (e.g., Teixeira and Hogan 2002; Bretherton et al. 2004a) clouds. The latter is dependent on the inversion intensity at the top of the boundary layer and is very difficult to simulate by stratiform cloud parameterizations. Some formulations are based on theoretical considerations, while others are more empirically derived from observational data. In addition, many of the schemes are based on the cloud-resolving model (CRM) and the large-eddy simulation (LES) model forced by observational data (e.g., Randall 1995; Xu and Randall 1996). The existence of these diverse cloud schemes is partly due to the effort to include progressively complex cloud physical processes into the cloud water parameterization, as well as the different basic assumptions one can choose to parameterize the cloudiness. Particularly, somewhat different (and ambiguous) definitions of sub-grid-scale cloudiness seem to contribute to the development of many cloud schemes.

These cloud parameterizations have been used in both operational NWP models and GCMs. For example, in the Third Hadley Centre Coupled Ocean–Atmosphere General Circulation Model (HadCM3), large-scale precipitation and cloud (Gordon et al. 2000) are formulated following Smith (1990). The Japan Meteorological Agency Global Spectral Model (JMA GSM) adopts a scheme based on Sommeria and Dardorff (1977), which is similar to Smith’s formula, but its microphysics are based on Sundqvist (1978) and Sundqvist et al. (1989). The National Centers for Environmental Prediction (NCEP) Global Forecast System (GFS) and Climate Forecast System (CFS) models have one cloud condensate as a prognostic variable (Sundqvist et al. 1989; Zhao and Carr 1997), and cloud amount is diagnosed from relative humidity and cloud condensate based on Xu and Randall (1996). In the European Centre for Medium-Range Weather Forecasts (ECMWF) Integrated Forecast System (IFS), both cloud condensate and cloud amount are predicted following Tiedtke (1993). For the cloud water, some models predict only a single cloud condensate while others have separate prognostic equations for cloud water, ice, and other cloud substances. The National Center for Atmospheric Research (NCAR) Community Atmosphere Model, version 3 (CAM3; Collins et al. 2006), includes both the prognostic cloud water and ice

equations (Boville et al. 2006); however, the stratiform cloud amount is diagnosed from relative humidity only. The Geophysical Fluid Dynamics Laboratory (GFDL) Global Atmosphere Model version 2 (AM2; The GFDL Global Atmospheric Model Development Team 2004; Delworth et al. 2006) includes both cloud water and ice (Rotstayn et al. 2000) and cloud amount as prognostic variables, based on Tiedtke (1993).

Improvements to the representation of clouds have lead to the improvement of weather forecasts and climate simulations. For example, Tiedtke (1993) showed that their prognostic cloud scheme realistically reproduced observed cloud cover and cloud water content, and increased the ECMWF global model skill. Fowler et al. (1996) implemented a more sophisticated prognostic cloud scheme into the Colorado State University (CSU) GCM and improved cloud–radiation feedback. Boville et al. (2006) noted that the predicted tropical tropopause temperature was greatly improved in CAM3 due to a better representation of cloud ice near the tropopause.

A major advantage of using prognostic equations for the cloud condensates is that cloud-driven radiation processes can be treated more physically, which is crucial for climate change simulations. Senior and Mitchell (1993) found that the presence or absence of cloud microphysical and optical thickness feedbacks could cause the global warming of surface temperature to vary from 1.9° to 5.4°C in their doubled-CO₂ experiments.

To identify the importance of cloud representation in GCMs, we will compare three conceptually different cloud water prediction schemes and cloud amount parameterizations associated with stratiform clouds using the Experimental Climate Prediction Center (ECPC) global-to-regional forecast system (G-RSM). It should be emphasized that the scope of this paper is limited to the impact of cloud parameterization on the seasonal mean field. We do not examine the model skill, because the transient and interannual behavior of the simulation requires long ensemble integrations of the order of 50 or more years for statistically meaningful results (Sardeshmukh et al. 2000), and we simply do not have sufficient resources to perform such integrations. We realize that the impact of parameterization on transient behavior, such as the simulation of interannual variability, is very different from what is expected of seasonal mean behavior.

The difficulties encountered in this comparison study are that the simulated cloudiness and associated radiation fluxes are extremely sensitive to some of the parameters used in the parameterization. It is an almost universal practice to “tune” the cloud schemes when adapted to a model. This tuning process is quite em-

pirical and sometimes even unphysical. It is commonly performed to match the model-produced radiation fluxes at the top of the atmosphere to satellite observations. It is also performed to match the radiation fluxes at the surface, although observation is not readily available, for the purpose of reducing the error in coupling with an ocean model. The tuning is also performed to make the simulated cloudiness agree with observation, but this is a little more involved because of difficulties in estimating the errors in the observed cloudiness. Another commonly performed tuning is the critical temperature for ice crystals formation, which often leads to unphysical tuning to compensate for temperature bias in the model. In operational forecast models, the tuning is mostly based on reducing the simulated temperature bias. The tuning process is quite tedious and expensive, because the simulations are a strong function of season and length of simulation, and may even vary from year to year. The tuning for temperature bias is even more difficult because it is a result of the complex interactions between various physical processes (and the atmospheric condition), which makes the estimation of the magnitude and direction of the tuning of parameters extremely difficult. We also note that the tuning is performed to reduce the seasonal mean bias of some target quantity, and no particular attention is paid to the skill of the model, namely, the simulation of high- and low-frequency transient disturbances. In our estimation this is the weakest point of the current tuning practice.

Considering the sensitivity of the simulation to tuning, and also the computational resource limitation, we have decided to minimize the tuning as much as possible, and we limited the tuning to those cases for which the simulation becomes significantly worse than others with known reasons. The Slingo cloud scheme based on relative humidity (RH), which is the default of the model, is specifically tuned for the model we used (Slingo 1987). In this scheme, the formulation of the relation between RH and cloudiness is determined empirically based on the model simulated RH and satellite cloud observation. We may argue that this scheme can be used as a benchmark for other schemes. This “no tuning” approach may be debatable, but we feel it can be justified from the following considerations. First, we believe that the parameterizations tested in this paper (with the exception of the Slingo scheme) are reasonably well based on physical principles, and thus, the parameters in all the schemes (except Slingo) are considered to be based on theory and/or observations; therefore, no tuning should be necessary. Second, from a practical point of view, unique (or universal) tuning is not possible because it cannot improve all the aspects

of the model simulation. For example, the improvement of outgoing longwave radiation may worsen the precipitation patterns or the simulation of the Madden-Julian oscillation (MJO). Third, a tuning made to one model may not be applicable to others. For those reasons, and to make this study as general as possible, we decided to keep the cloud parameterization schemes as close as possible to those originally published.

This paper is organized as follows: in section 2, the cloud parameterizations used in this study are presented; the observation and reanalysis data and the model and experiment setup are given in section 3; in section 4, experimental results are shown; in section 5, relationships between relative humidity, cloud amount, and cloud water are discussed; and conclusions are presented in section 6.

2. Cloud parameterizations examined in this study

Comparisons of the cloud parameterizations are complicated by the following separation of clouds into three distinctly different types in almost all of the large-scale models: 1) stratiform cloud, 2) convective cloud, and 3) inversion-topped boundary layer cloud. These three types of clouds are treated independently in most models, because one parameterization scheme is not able to properly simulate all of those cloud types. For example, boundary layer cloud, commonly observed over the coastal regions of the eastern Pacific and the Atlantic, cannot be realistically simulated by common stratiform cloud parameterizations (e.g., Dyuinkerke and Teixeira 2001), and a special parameterization is necessary. Similarly, convective cloudiness is also difficult to parameterize using stratiform cloud schemes. We realize that there may be strong interactions between these different types of clouds; however, it is beyond our resources to perform a combination of all of the different types of parameterizations. We confined our interest to the stratiform cloud type, and used the same cloud parameterizations for convective cloud and inversion-topped boundary layer cloud whenever possible. One advantage of this design is that we can study the interaction between the three different cloud types when the stratiform cloud parameterization is changed. The cloud parameterizations used for each of the four stratiform cloud schemes are summarized in Table 1.

We will first discuss the cloudiness associated with convective cloud (section 2a) and inversion-topped boundary layer cloud (section 2b), and then elaborate on the four stratiform cloud schemes (section 2c).

TABLE 1. Summary of cloud parameterizations.

| Code | No. of cloud water prognostic variables | Cloud water prognostic variables | Stratiform cloud | Convective cloud | Boundary layer cloud | Efficiency (%) (SLINGO = 100%) |
|--------|---|----------------------------------|--|---|--|--------------------------------|
| SLINGO | 0 | (None) | Diagnosed from RH (Slingo 1987) | Diagnosed from convective precipitation (Slingo 1987) | Diagnosed from inversion strength and RH (Slingo 1987) | 100 |
| ZC | 1 | q_c/q_i | Diagnosed from RH and qc/qi (Randall 1995) | Same as SLINGO | Same as SLINGO | 110 |
| IS | 1 | q_c/q_i | Predicted (Tiedtke 1993) | Predicted (Tiedtke 1993) | Same as SLINGO | 150 |
| HONG | 2 | $q_c/q_i, q_r/q_s$ | Same as ZC | Same as SLINGO | Same as SLINGO | 240 |

a. Cloudiness associated with convective cloud

The cloudiness associated with convective cloud, except in Iacobellis and Somerville (2000) [IS; see section 2c(3)], is based on Slingo (1987). The convective cloud amount (C_c) is a function of the model's convective precipitation rate (P_{cnv}) and takes the following empirical form:

$$C_c = 0.200 + 0.120 \ln P_{\text{cnv}}. \quad (1)$$

The coefficients in Eq. (1) were determined to fit observed cloudiness.

Additionally, for the Slingo scheme [section 2c(1)], anvil cirrus is assumed to form if $C_c \geq 0.3$ and the cloud top is higher than $\sigma = 0.4$, where σ is the vertical coordinate of the model (400 hPa, when the surface pressure is 1000 hPa). The cloud bases and tops are determined by the mass flux vertical distribution in the convective parameterization. The cloud amount (C) resulting from anvil cirrus is calculated as

$$C = 2(C_c - 0.3). \quad (2)$$

For the schemes with cloud water as a predictive variable, this somewhat artificial increase in upper-level cloudiness is turned off. Instead, the detrainment of

cloud water from the top of the convective cloud is added as a source of cloud water in the cloud water prediction equation. By doing so, the cloudiness calculation is left to the stratiform cloudiness parameterization.

b. Cloudiness associated with inversion-topped boundary layer cloud (marine stratus)

The stratus over cold ocean topped by strong atmospheric inversion is prevalent over the eastern Pacific and Atlantic (e.g., Bretherton et al. 2004b). This type of cloud, commonly called marine stratus, is essential for atmospheric and ocean interaction, but very difficult to simulate using the cloud physical processes currently incorporated into numerical models (e.g., Stevens et al. 2001, 2005; Duynkerke and Teixeira 2001; Bretherton et al. 2004a). The scheme used in this study is taken from Slingo (1987). When there is subsidence ($\omega \geq 0$) over ocean below 870 hPa, and if an inversion is present with $\partial\theta/\partial p \leq -0.055 \text{ K hPa}^{-1}$, we assume that the boundary layer clouds exist. The cloud amount is determined from the inversion intensity and relative humidity RH_B at the inversion base,

$$\begin{aligned}
 C &= 0, & \text{for } \text{RH}_B < 0.55 \\
 C &= \left(-16.67 \frac{\partial\theta}{\partial p} - 0.92 \right) \left(\frac{\text{RH}_B - 0.55}{0.25} \right), & \text{for } 0.55 \leq \text{RH}_B \leq 0.80 \\
 C &= \left(-16.67 \frac{\partial\theta}{\partial p} - 0.92 \right), & \text{for } \text{RH}_B > 0.80.
 \end{aligned} \quad (3)$$

This parameterization is used in all of the experiments performed in this study. It is noted that Eq. (3) is used with the IS scheme, although their cloudiness prediction equation includes the source from boundary layer clouds. This is because the boundary layer cloud is

deficient in the IS scheme. We found that the cloud coverage calculated from Eq. (3), and accordingly the low-level cloud coverage, is very sensitive to the specification of the allowable boundary layer top (870 hPa, in this study). For the purpose of comparison, we in-

tentionally left this parameter fixed without adjusting it to make the simulation fit better with observations.

c. Cloudiness associated with stratiform cloud

1) RELATIVE HUMIDITY–BASED SCHEME
(SLINGO SCHEME)

In the control simulation (SLINGO), the cloud amount is based on Slingo (1987). The stratiform cloud amount is formulated as

$$C = \left(\frac{RH - RH_c}{1 - RH_c} \right)^2, \quad \text{for } RH > RH_c \quad (4)$$

$$C = 0, \quad \text{for } RH \leq RH_c,$$

where RH is the mean relative humidity over the area represented by a grid, and RH_c is the critical value of relative humidity for the cloud to form, which is specified differently for each cloud layer (high, middle, and low) from the historical forecast to fit corresponding observed cloudiness. In this study, 0.85, 0.65, 0.85, 0.90, and 0.70 are used for high cloud over land and ocean, middle cloud over land, middle cloud over ocean, low cloud over land, and low cloud over ocean, respectively.

In our radiation calculation, cloud optical properties are a function of the cloud water path (CWP), which is assumed to be simply a function of temperature (Slingo 1989). Supersaturation is removed instantaneously as precipitation, and evaporation occurs when precipitation falls through the unsaturated atmospheric layers.

2) ZHAO AND CARR’S CLOUD WATER SCHEME

The simplest prognostic cloud water scheme used in this study is that of Zhao and Carr (1997; ZC), which was first developed by Sundqvist et al. (1989). The prediction equation of the cloud water/ice mixing ratio is

$$\frac{\partial q_c}{\partial t} = A(q_c) + S_c + S_g - P - E_c + D_{qc}, \quad (5)$$

where q_c is the cloud water/ice mixing ratio, $A(q_c)$ is the horizontal advection of q_c , and S_c and S_g are the sources of q_c from convection (subgrid scale) and stratiform (grid scale) clouds, respectively. Here, P is the precipitation production rate from the cloud water/ice mixing ratio, E_c is the cloud evaporation rate, and D_{qc} is the horizontal and vertical diffusion; S_c is the detrainment of cloud water from the top of the convective cloud specified by the convective parameterization; S_g is a function of the tendencies of specific humidity, tem-

perature, and pressure, and is zero when RH is less than the critical relative humidity (RH_b); and E_c brings RH closer to RH_b when RH is less than RH_b , but is zero otherwise.

The cloud cover b is determined by the equation (Sundqvist et al. 1989)

$$b = 1 - \left(\frac{1 - RH}{1 - RH_b} \right)^{1/2}. \quad (6)$$

When $RH < RH_b$, $b = 0$. In this study, RH_b is set to 0.85, based on sensitivity studies. It should be noted that the cloud coverage b is only used in the prediction equation for the cloud water/ice mixing ratio [Eq. (5)]. To calculate precipitation production rate P , the autoconversion of cloud water/ice to rain/snow, the correction of cloud substance by falling precipitation, and the melting of snow below the freezing level are taken into account. The autoconversion of cloud water to rain is parameterized following Sundqvist et al. (1989):

$$P_{\text{raut}} = c_o q_c \left\{ 1 - \exp \left[- \left(\frac{q_c}{q_{cr} b} \right)^2 \right] \right\}, \quad (7)$$

where constants c_o and q_{cr} are $1.0 \times 10^{-4} \text{ s}^{-1}$ and $3.0 \times 10^{-4} \text{ (kg kg}^{-1}\text{)}$, and b is from Eq. (6). The autoconversion of cloud ice to snow is parameterized following Lin et al. (1983):

$$P_{\text{saut}} = a_1 (q_c - q_{ci0}), \quad (8)$$

where q_{ci0} is the threshold mixing ratio of cloud ice to snow and is set to a value of $5.0 \times 10^{-6} \text{ (kg kg}^{-1}\text{)}$, which is smaller than the value in the original paper. Here a_1 takes into account the temperature effect on P_{saut} .

In the radiation, cloud amount is calculated using Randall’s (1995) formula:

$$C = RH \left[1 - \exp \left(\frac{-\alpha q_c}{1 - RH} \right) \right], \quad (9)$$

where constant α is 1000. Radiative properties of clouds are calculated using cloud water content. Cloud optical properties are a function of the CWP following Slingo (1989) for liquid water clouds, and Ebert and Curry (1992) for ice clouds. The effective cloud-droplet radius for liquid water cloud is parameterized following Wyser (1998), and for ice following Bower et al. (1994).

3) IACOBELLIS AND SOMERVILLE’S CLOUD SCHEME

The Iacobellis and Somerville (2000) cloud scheme, first proposed by Tiedtke (1993), predicts both the cloud water/ice mixing ratio and cloud amount. The

prediction equation for the cloud water/ice mixing ratio is

$$\frac{\partial q_c}{\partial t} = A(q_c) + S_c + S_{BL} + S_g - P - E_c + D_{qc}, \quad (10)$$

where S_{BL} is the source of cloud water/ice from the boundary layer, and S_c is the detrainment of cloud water from the top of the convective cloud. To calculate S_g , the tendency of saturation specific humidity by large-scale lifting and diabatic cooling is taken into account (Tiedtke 1993). In addition, S_g is set to zero when the mean relative humidity exceeds the pressure-dependent critical value, defined as 80% at 650 hPa and 100% at both the boundary layer top and the tropopause (Tiedtke 1993). Here S_{BL} , which is not included in the ZC scheme, is the turbulent moisture transport estimated in the boundary layer scheme. However, our experiment showed that the S_{BL} is too small in the boundary layer to form boundary layer clouds. Thus, it was necessary to add a separate parameterization for inversion-topped boundary layer clouds. This insufficiency of the S_{BL} term seems to be caused by the underestimation of turbulent moisture transports in the model's boundary layer parameterization. The following two processes make up E_c : large-scale descent and diabatic heating, and the turbulent mixing of cloud air and unsaturated environmental air. Precipitation processes for both cloud water and ice follows Sundqvist et al. (1989), similar to Eq. (7); however, c_0 and q_{cr} are variables to take into account the effect of the collection of cloud droplets falling through the cloud (the Bergeron–Findeisen process). The predicted cloud amount, which is described next, is used as b instead of Eq. (6) in the ZC scheme.

For cloud amount, the prediction equation is expressed as

$$\frac{\partial C}{\partial t} = A(C) + S(C)_c + S(C)_{BL} + S(C)_g - D(C), \quad (11)$$

where $A(C)$ is the horizontal advection of clouds; $S(C)_c$, $S(C)_{BL}$, and $S(C)_g$ are the formation of cloud area by convection, boundary layer turbulence, and stratiform cloud processes, respectively; and $D(C)$ is the rate of the dissipation of clouds. The terms $S(C)_c$, $S(C)_{BL}$, and $S(C)_g$ are calculated in a similar manner as S_c , S_{BL} , and S_g . Precipitation does not appear in Eq. (11), thus the cloud amount is not affected by precipitation.

Cloud radiative properties are calculated using the same parameterizations as ZC.

4) HONG'S CLOUD WATER SCHEMES

Hong's cloud schemes (HONG n , where n is the number of predicted water substances; Hong et al. 1998, 2004) utilize bulk parameterization as in Lin et al. (1983), Rutledge and Hobbs (1983), and Dudhia (1989). It predicts clouds and precipitation, but incorporates an improved ice process treatment (Hong et al. 2004). In this study, the three water substance prediction scheme (HONG3) is used because of its high efficiency. More complex versions of Hong's cloud schemes are also examined—HONG5 employs five prognostic species, including water vapor, cloud water, cloud ice, rain, and snow, and HONG6 employs graupel in addition to the previously mentioned five species. The results from using HONG3, HONG5, and HONG6 in global model simulations are very similar. However, HONG5 and HONG6 are much more expensive than HONG3 and were not used.

The HONG3 scheme has a rain/snow mixing ratio in addition to a cloud water/ice mixing ratio as prognostic variables. The model prediction equations for the cloud water/ice mixing ratio and the rain/snow mixing ratio are

$$\begin{aligned} \frac{\partial q_c}{\partial t} &= A(q_c) + F(q_c) + D_{qc}, \\ \frac{\partial q_r}{\partial t} &= A(q_r) + F(q_r) + D_{qr} - P, \end{aligned} \quad (12)$$

where q_r is the rain/snow mixing ratio, D_{qr} is the horizontal and vertical diffusion of q_r , and P is the sedimentation of falling precipitation droplets. Though the microphysical processes in this scheme represent only the $F(q_c)$ and $F(q_r)$ terms for the cloud water/ice mixing ratio and rain/snow mixing ratio, respectively, they contain the condensation of water vapor into cloud water and ice at saturation, the accretion of cloud by rain and ice by snow, the evaporation and sublimation of rain and snow, the initiation and sedimentation of ice crystals, and the sublimation or deposition of ice crystals.

The autoconversion of cloud water to rain is parameterized following Kessler (1969):

$$P_{\text{raut}} = a_2(q_c - q_{cr0}), \quad (13)$$

where a_2 and q_{cr0} are calculated based on the dynamic viscosity of air, the density of water, droplet concentration, the acceleration resulting from gravity, the mean collection efficiency, and the critical mean droplet radius where the autoconversion begins. For cloud ice-to-snow conversion,

$$P_{\text{saut}} = \max[(q_c - q_{ci0})/\Delta t, 0] \quad (14)$$

is used, where Δt is the length of the time step. The critical value of the autoconversion of cloud ice to snow q_{ci0} is temperature dependent.

The cloud amount parameterization is the same as that used in ZC and is calculated from Eq. (9). Cloud radiative properties are also in the same manner as ZC and IS.

d. Note on RH

There are some differences in the computation of relative humidity in the experiments, which may affect the result. In SLINGO, relative humidity is calculated with respect to water for all temperature ranges. This follows the procedure used in the NCEP–National Center for Atmospheric Research (NCAR) reanalysis and NCEP–Department of Energy (DOE) Atmospheric Model Intercomparison Project (AMIP-II) Reanalysis (R-2). Thus relative humidity in the upper troposphere and stratosphere may be in error and biased, but the relative change of relative humidity still represents the change in moisture content. In ZC, the relative humidity is computed by taking into account more detailed cloud physical processes. In the regions where $T > 0^\circ\text{C}$, there is no cloud ice and RH is calculated with respect to water, while in regions where $T < -15^\circ\text{C}$, no cloud water is allowed and RH is calculated with respect to ice. In regions between -15° and 0°C , if there are cloud ice particles above this level at the previous or current time step, or if the cloud at this point at the previous time step consists of ice particles, RH is calculated with respect to ice. Otherwise, all clouds in this region are considered to contain supercooled water and RH is calculated with respect to water. However, for the radiation process, RH is computed either on ice or water based on the temperature; thus, there is an inconsistency in the treatment of ice effect between the cloud water scheme and the radiation scheme in the ZC scheme. For the IS and HONG schemes, RH is computed appropriately according to the temperature.

3. Data, model, and experimental setup

a. Observational data

The International Satellite Cloud Climatology Project (ISCCP) D2 (Rossow and Schiffer 1999) data are used in this study. ISCCP D2 data are a monthly dataset in 280-km horizontal resolution. This dataset consists of cloud amount, cloud-top pressure, cloud-top temperature, cloud optical thickness, and CWP for 15 cloud types during the daytime. The cloud types are defined by cloud-top pressures and cloud optical thicknesses. In addition, low and middle clouds are divided into liquid and ice phase clouds (high clouds are as-

sumed to be ice clouds). Cloud amount and CWP are used in this study. For simplicity, the 15 cloud types are combined into the following 3 cloud types: low (defined by cloud-top pressure $P_c > 680$ hPa), middle ($440 < P_c \leq 680$ hPa), and high ($P_c \leq 440$ hPa).

The relative humidity is taken from R-2 (Kanamitsu et al. 2002a). Maximum relative humidity in each cloud layer is used, and then interpolated to the ISCCP grid. This relative humidity is computed with respect to water at all the temperatures.

Monthly data from the ISCCP and R-2 for the 10-yr period from 1990 to 1999 were used in this study. The data in the area from 60°S to 60°N are used because cloud-detection errors are known to be large in the ISCCP polar region (Rossow and Schiffer 1999).

For precipitation, the Global Precipitation Climatology Project (GPCP), version 2, monthly precipitation dataset (Adler et al. 2003) is used. The Earth Radiation Budget Experiment (ERBE) dataset and the Surface Radiation Budget (SRB) dataset (Stackhouse et al. 2004) are used for radiation at the top of the atmosphere (TOA) and at the surface (SFC), respectively. In this study, the period of the ISCCP, GPCP, SRB, and R-2 data is from 1990 to 1999, matching that of the experiment, while ERBE is from the 1985 to 1989 period. We believe the comparison is valid because it is made for the long-term mean.

b. Model

The global model version of the ECPC G-RSM is used in this study, which is based on the NCEP Seasonal Forecast Model (SFM; Kanamitsu et al. 2002b). The horizontal resolution is T62 and has 28 sigma levels in the vertical. The physics in the ECPC G-RSM include the relaxed Arakawa–Schubert convection scheme (Arakawa and Schubert 1974; Moorthi and Suarez 1992) as deep convection, shallow convection, nonlocal boundary layer vertical diffusion (Hong and Pan 1996), shortwave (Chou 1992) and longwave (Chou et al. 1999) radiation parameterizations, and the Noah land surface model (Ek et al. 2003). The stratiform cloud schemes used in this study were described in section 2c.

High, middle, low, and total cloud amounts from model simulations were calculated using maximum-random overlap assumption (Chou et al. 1998). Note that the model's cloud data may not be directly compared with the ISCCP cloud data because they are based on a view from space, and lower clouds could be sheltered by upper clouds (e.g., Weare 2000, 2004). For the purpose of comparing the model's three layered cloud amounts with the ISCCP, the model cloud amounts are transformed to ISCCP D2 comparable estimates fol-

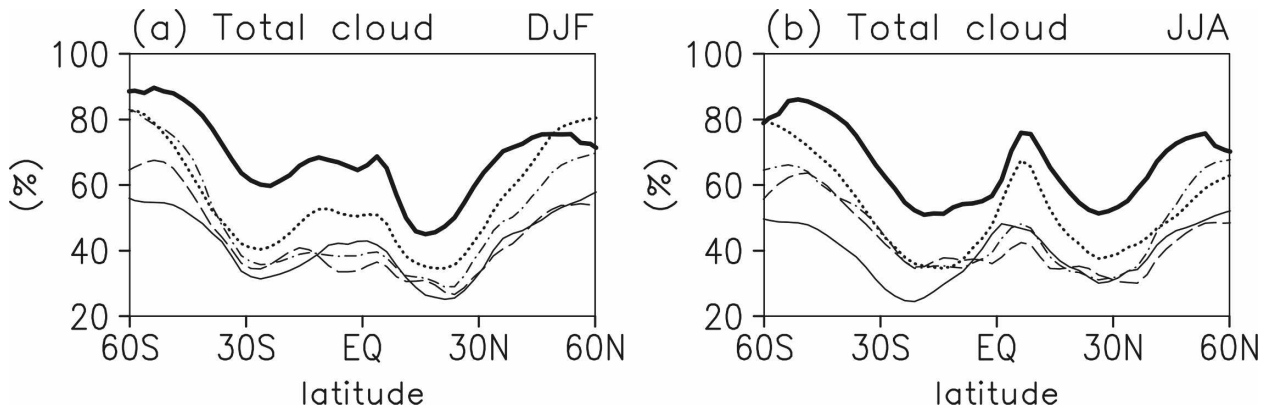


FIG. 1. Zonally averaged distributions of observed and simulated total cloud amount (%) in (a) DJF and (b) JJA for 1990–99. ISCCP (thick solid line), SLINGO (thin solid line), ZC (dashed line), IS (dotted line), and HONG (dot-dashed line) are shown.

lowing Weare (2004). For the model high cloud, the amount should be the same as that observed from space. The model middle cloud amount as observed from space is the amount of the middle cloud not sheltered by high cloud. Using the “random overlap assumption”, the corrected middle cloud amount mid_asfa_cf will be expressed as

$$mid_asfa_cf = mid_cf \times (1 - high_cf), \quad (15)$$

where $high_cf$, mid_cf are the model high and middle cloud amounts. Similarly, the corrected model low cloud amount low_asfa_cf is defined as

$$low_asfa_cf = low_cf \times (1 - mid_cf) \times (1 - high_cf), \quad (16)$$

where low_cf is the model low cloud amount. It should be noted that these corrected cloud amounts should only be used for comparison with ISCCP data, but not for comparing cloud amounts between the models. The CWP from the model simulations was calculated using the cloud water/ice mixing ratio.

The model simulations were performed from January 1989 to December 1999, but the first year is excluded from the evaluation. The simulations were started from the R-2 analysis, and the model was integrated using observed daily sea surface temperatures (SSTs), which were interpolated from the NCEP weekly analysis (Reynolds and Smith 1994).

4. Results

a. Clouds

Figure 1 compares the zonally averaged total cloud amount distribution for December–February (DJF) and June–August (JJA). All simulations have their total cloud amount peaks in the low and midlatitudes in

both DJF and JJA, agreeing with observations, but with a clear bias of more than 20% in most of the latitudes. Some schemes are better in some latitudes and seasons, while other schemes are better in others. Among the

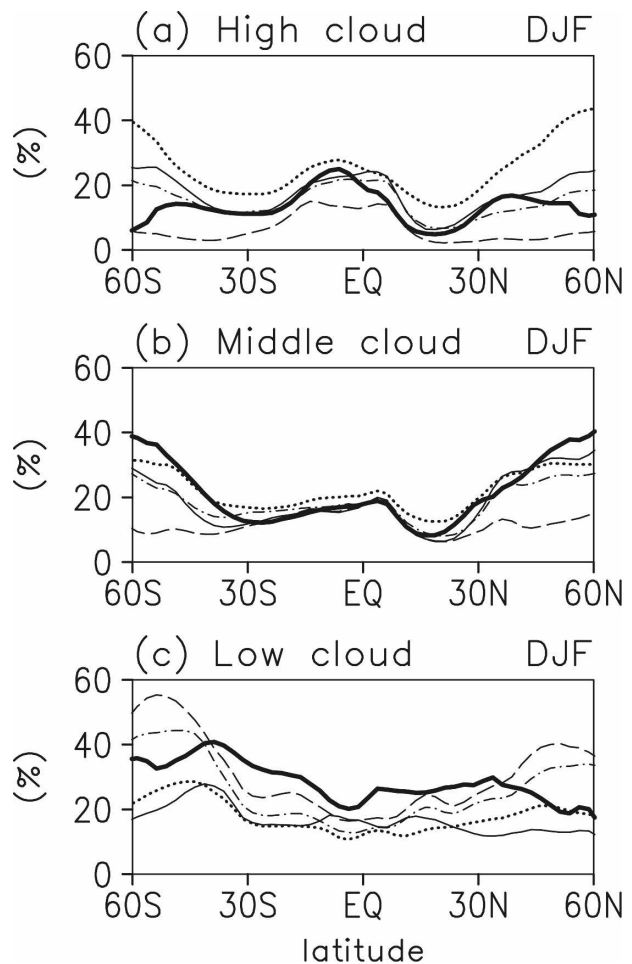


FIG. 2. As in Fig. 1, but for (a) high, (b) middle, and (c) low cloud amount in DJF.

four schemes, IS shows a somewhat better total cloud distribution than the other cloud schemes.

Zonally averaged high, middle, and low cloud amount distributions for DJF are shown in Fig. 2. For this verification, the corrected cloudiness as viewed from space is used for comparison with that of ISCCP [Eqs. (15) and (16)]. The result for JJA was very similar (not shown). High cloud amounts are better simulated in SLINGO and HONG, overestimated in IS, and underestimated in ZC. For middle clouds, all simulated cloud amounts are in good agreement with the ISCCP in low latitudes, while they are underestimated in high latitudes. For the low clouds, cloud amounts are underestimated in low latitudes, but are overestimated in IS and HONG, and underestimated in SLINGO and ZC in other latitudes. The underestimation of low cloud amounts in low latitudes and the underestimation of middle cloud amounts in high latitudes are consistent with the underestimation of simulated total cloud amounts in the extratropics.

Those cloud distributions are very sensitive to the empirical parameters used in each cloud scheme and adjustment of the parameter can reduce the zonal bias. For example in ZC, the negative bias in high clouds is related to the low cloud ice content, which is very sensitive to the critical value used for the autoconversion. However, improvement of spatially varying bias is much more difficult.

Looking at the geographical distribution of high cloud amount (Fig. 3), it is clear that the pattern in the tropics is fairly similar in all the cloud schemes. Further examination showed that the high cloud amount distribution resembles the relative humidity distribution in all cloud schemes (not shown). This will be discussed further in section 5. We also found that the cloud ice content affects both the cloud amount distribution and the simulated temperature field through cloud radiation interaction. This topic will be covered in section 4c.

To compare the low-level clouds between the four cloud schemes, observed and simulated JJA low cloud amounts are shown in Fig. 4. Note again that the model raw cloud amount (*low_cf*) is used for comparison of simulated model clouds. Though an underestimation of low cloud amounts is again seen in low latitudes, ZC, IS, and HONG are apparently better than SLINGO. This minor improvement is found over subtropical ocean (Fig. 4), suggesting that the cloud water scheme improves low cloud amounts because of either the simulated low-level cloud water or the interaction between the stratiform and boundary layer clouds. This improvement is also seen over land in NH midlatitudes in JJA (Fig. 4), where relative humidity is low. The 90% critical relative humidity for the formation of low cloud

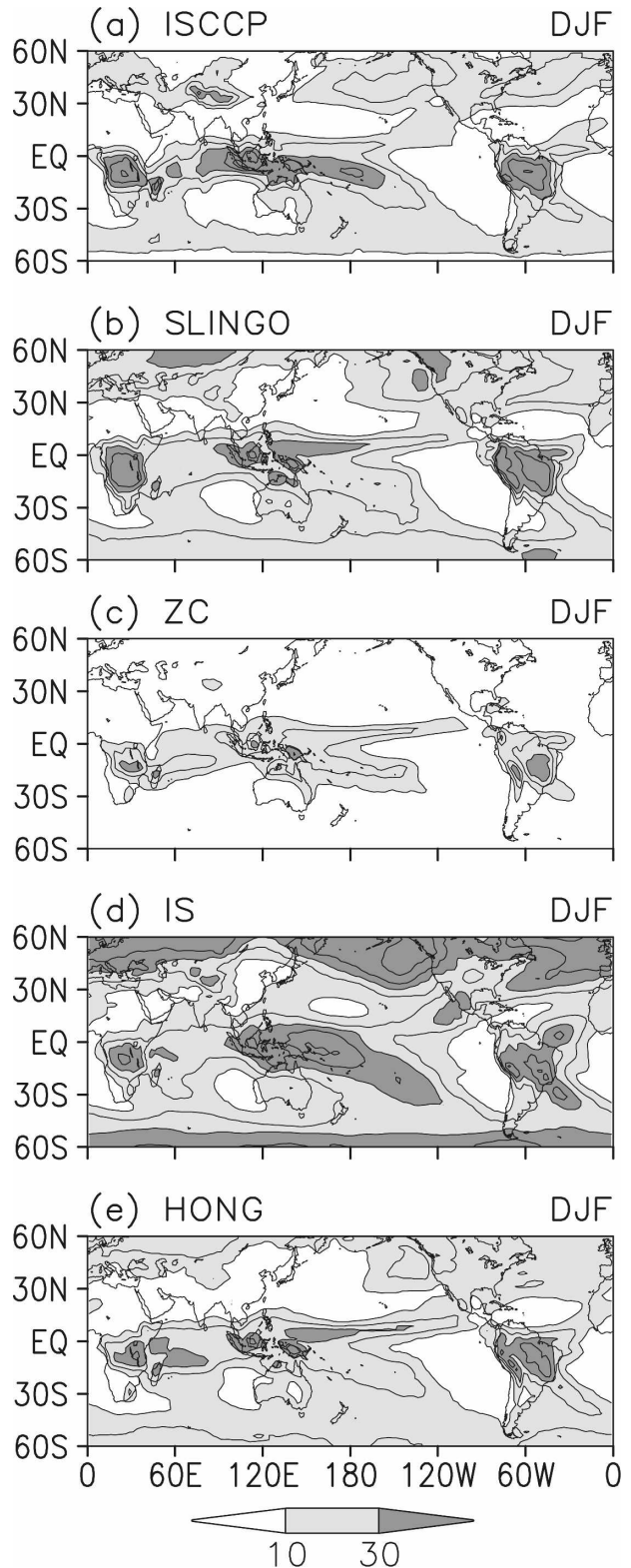


FIG. 3. Geographical distributions of observed and simulated high cloud amount (%) in DJF for 1990-99: (a) ISCCP, (b) SLINGO, (c) ZC, (d) IS, and (e) HONG. Contour interval is 10%. Light stippled area is for 10% to 30% and heavy stippled for >30%.

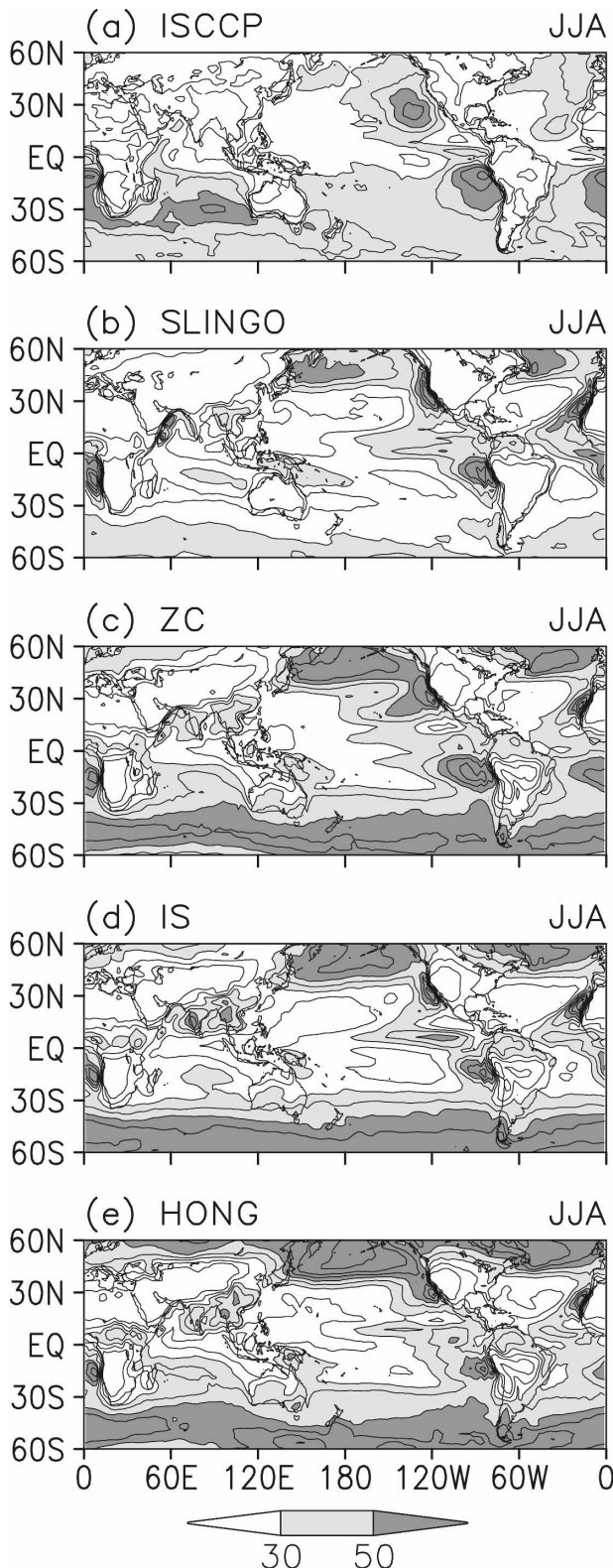


FIG. 4. As in Fig. 3, but for low cloud amount in JJA. Here, light stippled area is for 30% to 50% and heavy stippled for >50%.

amount over land in SLINGO is too high during summer, resulting in negative bias. Incorporating cloud water prediction improves such cases.

Figure 5 shows zonally averaged CWP distributions for ISCCP, ZC, IS, and HONG, respectively. CWP is mostly overestimated, except in NH midlatitudes for ZC and HONG in DJF. This overestimation is caused by the overestimation of CWP associated with water (liquid) clouds, which are 3–4 times larger than observed (Fig. 5d). The CWP associated with ice clouds is better simulated, however, it is overestimated in IS and underestimated in ZC. HONG produced better CWP associated with ice clouds than IS and ZC in this study.

b. Precipitation

Zonally averaged precipitation distributions in DJF and JJA (Fig. 6) show that simulated precipitation is overestimated in low latitudes for all simulations. Two precipitation peaks appear in the tropics, indicating a double intertropical convergence zone (ITCZ). This ITCZ pattern is a common problem seen in many GCMs (e.g., Covey et al. 2003; Dai 2006). In the mid- and high latitudes, simulated precipitation agrees well with observation. From the geographical distribution of precipitation (Fig. 7), IS is the best of all the cloud schemes, especially in low latitudes. Particularly, the relative magnitude of precipitation between ITCZ and the South Pacific convergence zone (SPCZ) is closer to observation than the other cloud schemes, though the amount of precipitation is still overestimated. It is surprising that the change in stratiform cloud parameterization strongly impacts the convective precipitation patterns in low latitudes.

c. Temperature

Figure 8 shows the zonally averaged vertical cross section of the DJF temperature difference between R-2 and each cloud scheme. In general, cold biases exist in the stratosphere that are not sensitive to cloud schemes in all experiments. In the troposphere, all simulations show fairly small temperature errors, especially in low latitudes, where the temperature error is under 2°C . In the extratropics, a warm bias appears in the upper troposphere, especially in ZC and IS near the tropopause in the summer hemisphere, which may be related to low cloud ice content and associated cloud radiative properties. In our sensitivity test, the warm bias seen in ZC is much worse in the simulation when the default autoconversion critical value of cloud ice to snow quoted in the original paper (Zhao and Carr 1997) is used. In the current simulation, a smaller critical value is used to reduce the warm bias. The amount of cloud water and

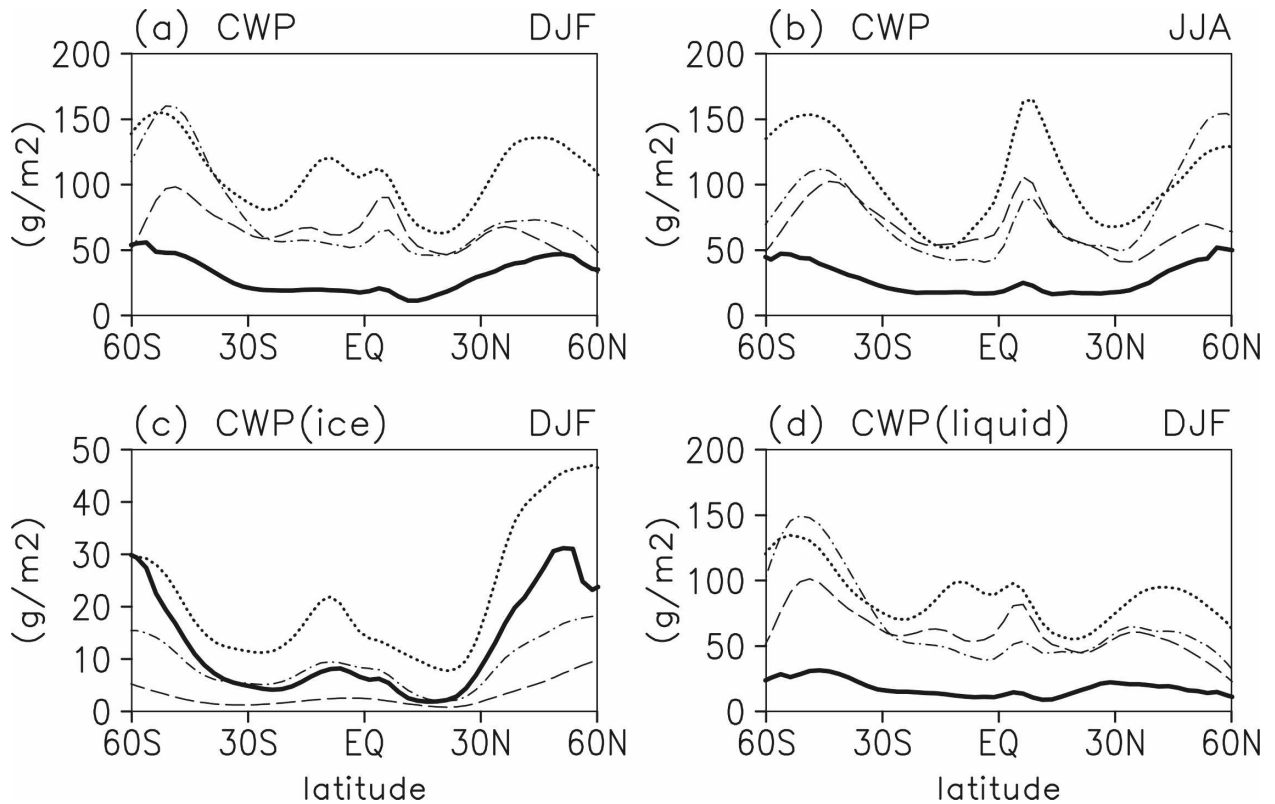


FIG. 5. As in Fig. 1, but for cloud water path (g m^{-2}) in (a), (c), (d) DJF and (b) JJA. (a), (b) All clouds, (c) ice clouds, and (d) water (liquid) clouds: ISCCP (thick solid line), ZC (dashed line), IS (dotted line), and HONG (dot-dashed line).

ice may not be the only cause of the warm bias, because the warm bias does not appear in HONG, in which the amount of CWP is similar to IS in the summer hemisphere (Fig. 5).

d. Radiation

Figure 9 shows the comparison of observed and simulated upward longwave and shortwave radiation fluxes (LWu, SWu) at the TOA, and downward longwave and shortwave radiation (LWd, SWd) at the SFC for DJF.

The LWu at the TOA (Fig. 9a) in IS has the smallest bias compared with ERBE, especially in the midlatitudes. Those biases are strongly related to high cloud distributions (Fig. 2a). However, because the high cloud amount in IS is overestimated, we think that the underestimation of longwave emissivity from CWP, or the underestimation of CWP itself in the model, is compensated by the overestimation of cloud amount. In addition, the cloud-top height and temperature also affects the simulated TOA LWu. In this context, an im-

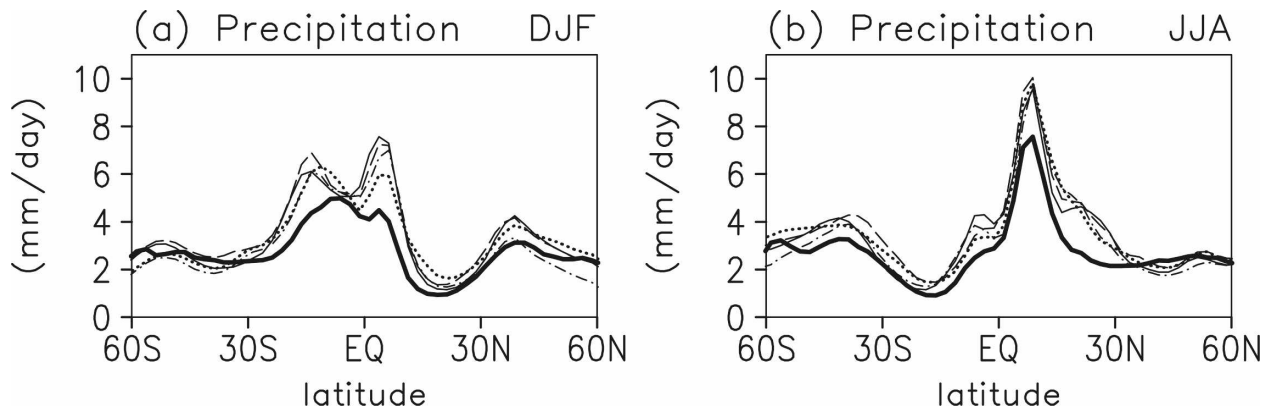


FIG. 6. As in Fig. 1, but for precipitation (mm day^{-1}). Observation is from GPCP.

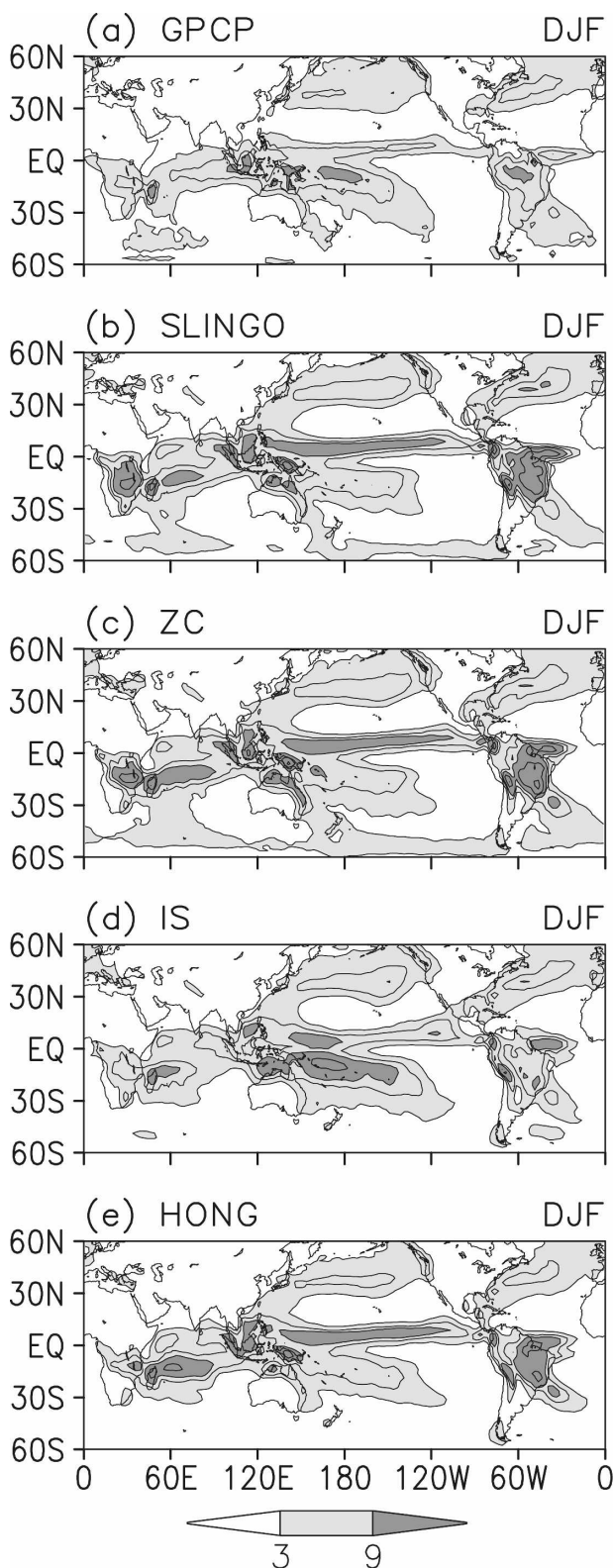


FIG. 7. As in Fig. 3, but for precipitation (mm day^{-1}) in DJF: (a) GPCP observed, (b) SLINGO, (c) ZC, (d) IS, and (e) HONG. Contour lines are 3, 6, 9, 15, and 21 mm day^{-1} . Light stippled area is for $3\text{--}9 \text{ mm day}^{-1}$ and heavy stippled for $>9 \text{ mm day}^{-1}$.

provement of clouds associated with convection and CWP seems to be needed.

SFC LWd (Fig. 9c) shows an opposite bias to that of TOA LWu. All cloud schemes show a common negative bias of about 20 W m^{-2} in low latitudes, while the error varies for each cloud scheme in midlatitudes. Those biases in the simulations are strongly related to low cloud distributions (Fig. 2c). It is clear that changing stratiform cloud schemes does not significantly improve the underestimation of SFC LWd in low latitudes.

In the tropics, TOA SWu is overestimated in IS, while it is underestimated in the others. In all of the cloud schemes, the area of large SWu bias roughly matches the area of large convective precipitation, suggesting that the stronger sensitivity of convective cloudiness to precipitation rate is needed to reduce the bias. In midlatitudes, it is clear that all of the cloud schemes except SLINGO simulate TOA SWd well. We also observe that SFC SWd is improved in those cloud schemes. We think this is due to the explicit prediction of cloud water in those cloud schemes, which allows more physical estimation of the cloud radiative property. Note that SLINGO does not predict cloud water, and the cloud radiative property is simply assumed as a function of temperature. Looking at the detail, although the ZC TOA SWu agrees with observation in most of the latitudes, it has a large error around 60°S similar to that of SLINGO. This is considered to be due to less high and middle cloud amounts around 60°S (Fig. 2).

e. Differences of formulations

In this section, we try to interpret the differences presented above from the difference in the formulation of cloud water and cloudiness prediction. Particularly, we will focus on the treatment of cloud ice. The autoconversion of cloud ice to snow and falling ice are the two processes that affected the mean cloud ice fields. In ZC and IS, autoconversion of cloud ice to snow is formulated as Eqs. (8) and (7), respectively. However, the effect of falling ice is not included. In contrast, HONG considered both the autoconversion and falling ice. As shown in Fig. 5c, HONG predicted better ice CWP distribution than ZC and IS. However, it is inconsistent that ZC produced lower cloud water (ice) content without considering the effect of the falling ice. As shown in Eq. (8), the threshold value of cloud ice to snow is smaller than that in the original paper. This mimics the effect of falling ice and, as a result, the cloud ice distribution improves. It should be noted that the parameter value used in Eq. (8) is unrealistically low, which caused the underestimation of ice CWP compared to ISCCP (Fig. 5c).

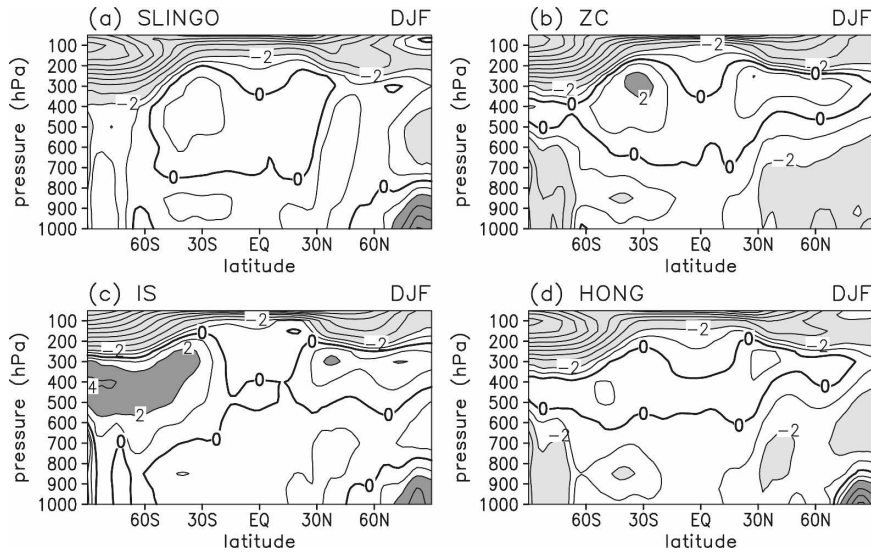


FIG. 8. Zonally averaged temperature differences (K) from R-2 for (a) SLINGO, (b) ZC, (c) IS, and (d) HONG in DJF for 1990-99. Contours indicate ± 1 K and then are at every 2 K. Area of light stippling is for <-2 and heavy stippling is for >2 .

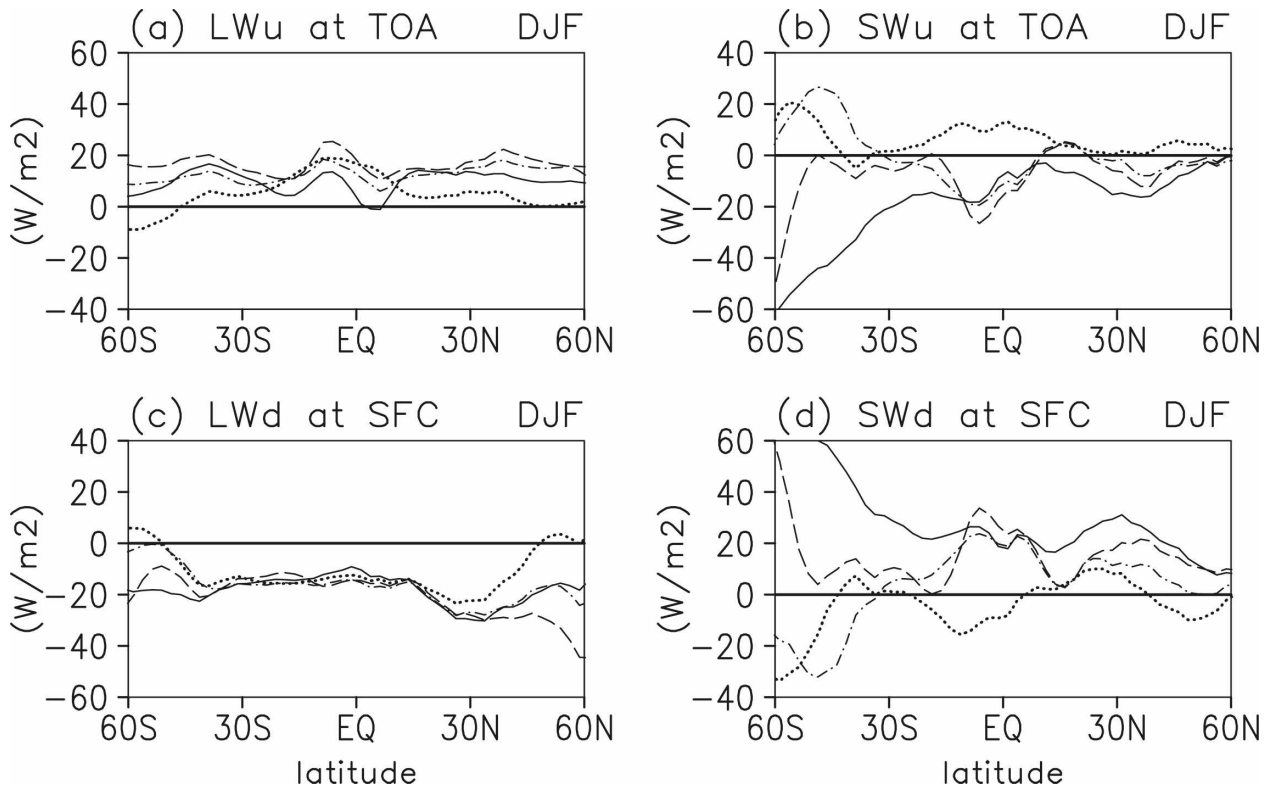


FIG. 9. Differences of zonally averaged radiation fluxes ($W m^{-2}$) between simulation and observation in DJF: (a) upward longwave radiation flux at TOA, (b) upward shortwave radiation flux at TOA, (c) downward longwave radiation flux at SFC, and (d) downward shortwave radiation flux at SFC. SLINGO (thin solid line), ZC (dashed line), IS (dotted line), and HONG (dot-dashed line). Observed radiation fluxes are from ERBE for TOA and SRB for SFC. The period of observation is 1990-99 for SRB and 1985-89 for ERBE.

In IS, both the cloud ice and high cloud amounts were overestimated. This may be because IS did not consider the falling ice. In addition, from Eq. (11), the cloud amount does not change when precipitation occurs in IS, while it decreases in ZC and HONG [from Eq. (9)] through the decrease of cloud ice. The relation between precipitation and cloudiness needs to be investigated from observations. The treatment of detrainment from convective clouds in IS is also different from that in ZC and HONG. From Eq. (11), detrainment from convective clouds directly increases cloud amount in IS, while the change of cloud amount is more complex in ZC and HONG because the cloud amount is estimated from the distribution of cloud water (ice) content and relative humidity, which are both predicted. Note that the cloud water (ice) in IS does not always increase when the cloud water is detrained because evaporation and precipitation also control them. The above processes may also be related with the transition from convective (subgrid scale) to stratiform (grid scale) clouds, and may be a more physically difficult subject.

f. Summary of the comparison of cloud schemes

In summary, the four stratiform cloud schemes show an underestimation of total cloud amount. The distributions of high, middle, and low cloud amounts for each cloud scheme are somewhat similar to observation, but with many disagreements. The distributions are very sensitive to physical parameters used in the cloud scheme. There is an indication that the prediction of cloud water improves the simulation, particularly over dry areas, but the improvement is minor. The stratiform cloud scheme affects convective precipitation distribution. All of the simulations suffer from systematic temperature error, which is also sensitive to the parameters in the cloud scheme, particularly to the autoconversion critical value of cloud ice to snow. The TOA and SFC radiation fluxes show that no cloud scheme stands out in all aspects, but some advantage is found for schemes in which predicted cloud water interacts with radiation. Simulated SW radiation fluxes are improved when a cloud water scheme is used; however, biases in LW radiation fluxes are still large in many of the schemes.

Although the IS scheme outperforms the other schemes in some respects, its advantage is small. Thus, we are forced to conclude that no one cloud scheme is better than others in all respects, and it is very difficult to arrive at any clear conclusions regarding which scheme to choose. This conclusion is under the constraint that the scheme did not undergo a rigorous tuning process, but even with tuning, it may not be possible

to arrive at general conclusions that apply to all situations and models because the cloud scheme may behave differently in different situations and modeling systems. This is somewhat in contrast to other parameterization schemes, such as convection, which are parameter dependent but much less sensitive than cloud parameterization.

5. Relationships between relative humidity, cloud amount, and cloud water

From the results obtained above, it becomes clear that the pattern of simulated cloud amount is strongly controlled by the relative humidity in mid- and high latitudes where stratiform clouds are dominant, especially for high clouds. Of course this is true for SLINGO, but it is also true for the schemes with cloud water prediction, for which cloud amount is a function of cloud water and relative humidity (with the exception of the IS scheme), because the cloudiness is formulated in such a way that it depends more strongly on relative humidity. In fact, Eq. (9) is formulated to increase cloud amount as relative humidity increases when cloud water is constant, and to increase the dependency of cloudiness to relative humidity when the cloud water content is small (Randall 1995; Xu and Randall 1996).

Some statistical relations between relative humidity and cloud amount have been investigated (e.g., Saito and Baba 1988; Teixeira 2001). The relationship between cloud amount, relative humidity, and cloud water was first proposed by Randall (1995), which is based on a cloud-resolving model simulation. The cloudiness is computed as a function of simulated spatially averaged relative humidity and cloud water, by assuming cloud formation when the cloud water exceeds a predetermined size. We have decided to reexamine this relationship based on ISCCP data, which is a large-scale observation and potentially more valid for coarse-resolution model parameterization. For this purpose, we generated several scatter diagrams of the relation between cloud amount, cloud water content, and relative humidity for high, middle, and low clouds from model simulations and from the combination of ISCCP observation and NCEP/DOE reanalysis. For cloud observation, the three-layered cloud amount and CWP from ISCCP were used. For simulations, CWP at each cloud layer was calculated from the output of cloud water content at pressure levels. Maximum relative humidity in each cloud layer was used for the relative humidity corresponding to low, middle, and high clouds, and then interpolated to the ISCCP grid for both the NCEP/DOE reanalysis and the simulations. The range of pressure levels for high, middle, and low

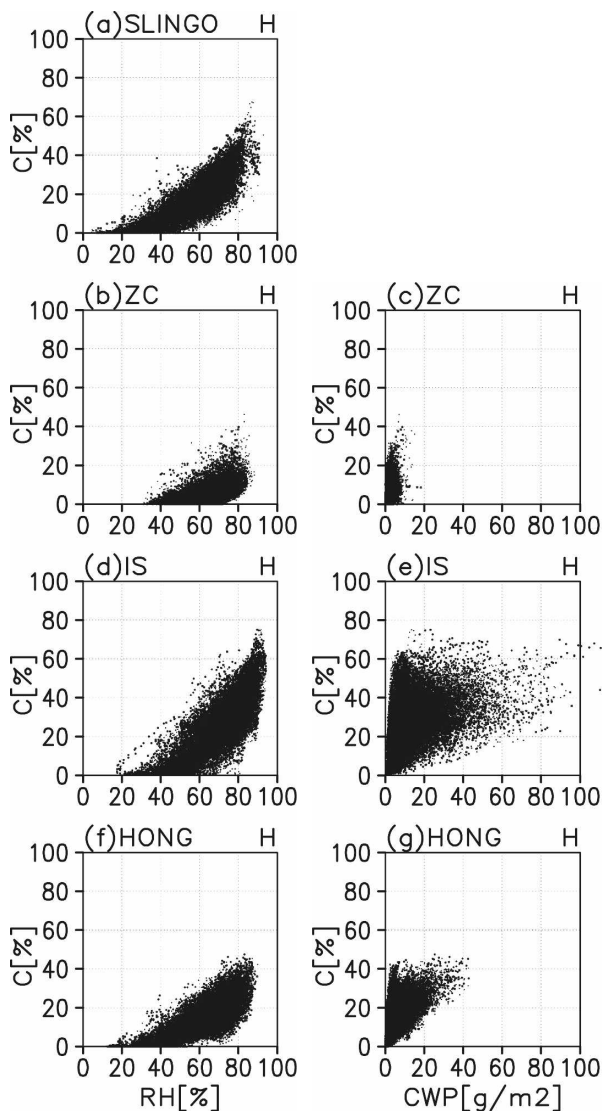


FIG. 10. Scatter diagrams of (left) relative humidity (%) vs cloud amount (%) and (right) cloud water path (g m^{-2}) vs cloud amount for high cloud from: (a) SLINGO; (b), (c) ZC; (d), (e) IS; and (f), (g). Simulations over the area (30° – 60°N , 0° – 360°) during January 1999–December 1999.

clouds were taken from ISCCP definitions. These pressure layers roughly correspond to the cloud layers in the ECPC G-RSM. Scatter diagrams of cloud water versus cloud amount and relative humidity versus cloud amount were made using monthly mean data. To limit our attention to stratiform clouds, we restricted the domain to 30° – 60°N . Similar computations were made in SH midlatitude and the results were very similar.

Figure 10 shows the scatter diagrams of cloud amount against relative humidity and cloud amount against cloud water for high cloud in model simulations. SLINGO has only one plot for relative humidity versus

cloud amount in Fig. 10 because cloud water is not predicted. The clouds include convective clouds, which are not dependent on relative humidity, and their contribution on high clouds may be small in midlatitudes. The figure indicates that in all model simulations, there is a tendency that when the relative humidity increases, the cloud amount also increases. The sensitivity of cloud amount to relative humidity (the derivative of the relation between RH and cloud amount with respect to height) is different for each simulation. IS shows the highest sensitivity of RH to cloudiness among the four simulations, while HONG and SLINGO have about the same sensitivities; ZC is less sensitive than the others. The lower sensitivity of ZC compared to HONG can be explained by the smaller cloud ice in ZC. The range of relative humidity and cloud amount is different for different cloud schemes. Sensitivities of cloud amount to cloud water are also different among the parameterizations. The range of CWP in ZC is small and the range of cloud amount for a given amount of cloud water is large, about 40%. In IS, the range of CWP is larger and the sensitivity of cloud amount to a given amount of cloud water is smaller compared to ZC. HONG shows higher sensitivity than IS. This sensitivity difference seems to be caused by the different methods for calculating cloud amount.

The corresponding scatter diagram from ISCCP observation is shown in Fig. 11. In making these figures, cloud amount and CWP for high thick cloud were not used because most of the high thick cloud is categorized as deep convection (Rossow and Schiffer 1999). It is clear that the range of cloud amount against a given relative humidity is larger in observation than in the simulations. For middle and low clouds, there is a tendency that when the relative humidity increases, cloudiness increases, but the range of cloud amount against relative humidity is much larger than in the simulations and the scatter is large (not shown). In contrast, there is a strong relation between cloud water and cloud amount, that is, the range of cloud amount against given cloud water is narrower than those seen in the relationships between relative humidity and cloud amount.

Apparently, the scatter diagrams showed that in the current cloud schemes, cloud amount is too dependent on relative humidity, while in reality it depends more strongly on cloud water. Based on this observation, we could consider using a diagnostic cloudiness scheme based only on cloud water. Our first attempt to test this method, however, failed. The simulation of cloudiness was much worse than the original formulation, the reason being the significant bias and poor skill in simulating cloud water. In fact, the introduction of relative

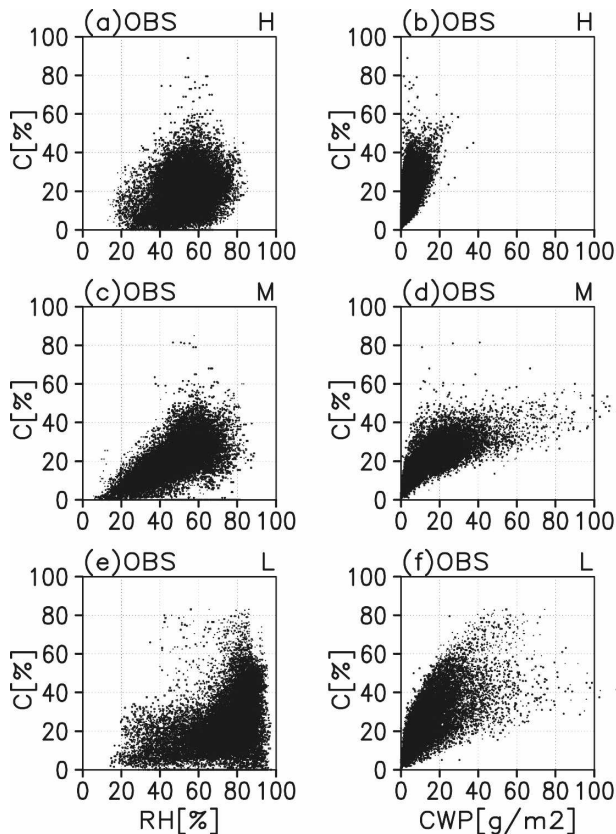


FIG. 11. Scatter diagrams of (left) relative humidity (%) vs cloud amount (%) and (right) cloud water path (g m^{-2}) vs cloud amount for (a), (b) high, (c), (d) middle, and (e), (f) low clouds from observation (ISCCP) and reanalysis (R-2) over the area (30° – 60° N, 0° – 360°) during January 1999–December 1999.

humidity for calculating cloudiness is a very clever way to reduce the sensitivity of cloudiness to cloud water, which is very poorly simulated by many of the current models. The message we received from these preliminary experiments is that the most crucial part of the cloud parameterization is the need to increase the accuracy of cloud water simulation, probably by an order of magnitude. If we can simulate cloud water more accurately, not only for stratiform cloud but also for convection and boundary layer topped clouds, then it may even be possible to use just one formulation of cloudiness based on cloud water, eliminating the need for separating the cloud parameterizations into three types (stratiform, convection, and boundary layer-topped clouds). Of course, in order to make this happen, we need to refine the cloud water prediction in all situations that range from marine boundary layer to deep convection.

It should be mentioned that in this study, relative humidity from the reanalysis (R-2) is used to estimate the relation between cloud amount and relative humid-

ity. The R-2 (and NCEP–NCAR reanalysis) does not distinguish the saturation vapor pressure over water and ice (R-2 always uses saturation over water), which introduces significant error in the value of relative humidity at low temperatures. Because observations of relative humidity at the upper troposphere (and stratosphere) are not abundant, and therefore the accuracy of the reanalysis is uncertain, arguing the relation between relative humidity and cloudiness at low temperatures may be problematic. Recently, Gettelman et al. (2006b) presented that relative humidity at low temperatures can be obtained from satellite observations. Gettelman et al. (2006a) examined supersaturated regions in the upper troposphere and showed that they are very frequent in the extratropical upper troposphere. These studies may be useful to examine relative humidity–cloudiness relationships further. In 2002, the first physical ice microphysics scheme for large-scale models was published (Kärcher and Lohmann 2002). Recently, some physically based parameterizations for ice clouds were suggested by Kärcher et al. (2006). However, our knowledge of ice cloud in the upper troposphere is far from satisfactory and its parameterization requires further effort.

6. Conclusions

In this study, four stratiform cloud parameterizations are compared by examining the seasonal mean fields forced by the observed SST using the ECPC G-RSM. We focused our attention on stratiform cloud, and therefore all other physical processes are fixed, including cloud parameterizations for convective clouds and inversion-topped boundary layer clouds. The simulated fields are compared to observation and reanalysis data, including ISCCP for clouds, GPCP for precipitation, ERBE and SRB for radiation, and R-2 for temperature. The following four cloud schemes are examined: 1) the Slingo scheme (SLINGO), in which cloud amount is diagnosed only from relative humidity; 2) the Zhao and Carr scheme (ZC), which has the cloud water/ice mixing ratio as a predictive variable, while the cloud amount is diagnosed from relative humidity and the cloud water/ice mixing ratio is based on Randall's (1995) formula; 3) the Iacobellis and Somerville scheme (IS), which predicts both the cloud water/ice mixing ratio and the cloud amount; and 4) the Hong scheme (HONG), in which the rain/snow mixing ratio and the cloud water/ice mixing ratio are predicted. The cloud amount is diagnosed from relative humidity, and the cloud water/ice mixing ratio is based on Randall's formula.

No stratiform cloud parameterization is found to per-

form better than others in all respects in simulating observed cloudiness, radiation, and the atmospheric temperature structure. This result may be strongly influenced by the fact that no special tuning was performed to improve the simulation (except for some schemes, which resulted in very large systematic errors). Considering that the simulation is very sensitive to parameters such as the critical value of cloud ice for autoconversion to snow, and inclusion of the falling velocity of ice in cloud schemes, it is very difficult to choose one particular stratiform cloud scheme using our approach, because every scheme can be *tuned* to perform better. Of course, it is not possible to improve all aspects of a model by tuning. Therefore, it may theoretically be possible to compare cloud schemes after tuning for some particular parameters (such as the radiation fluxes). However, such a practice may not be scientifically fruitful or useful, because the tuning is definitely dependent on models as well as initial conditions, and the applicability of the results to other models and other situations may be questionable. We note that this strong sensitivity of the cloud to parameters used in parameterization is somewhat in contrast to convective parameterization, which is less sensitive to changes in parameters.

Considering these limitations, we decided to look at those results with more general implications, which are summarized as follows:

- 1) The simulated cloudiness is more or less the same for all the schemes. Only the IS scheme, which predicts cloudiness, seems to distinguish itself from the others, but the improvement is small.
- 2) The simulated cloud water distribution is more or less the same for ZC, IS, and HONG. The inclusion of more complex cloud physics does not significantly change the cloud water distribution.
- 3) The incorporation of cloud water produces more clouds in dry areas, indicating that those schemes may have more general applications.
- 4) There is a strong interaction between parameterized stratiform clouds, boundary layer clouds, and convective clouds. On many occasions, the boundary layer cloud dominates the total cloud cover, which is important for atmosphere–ocean coupled modeling.
- 5) There is a strong interaction between parameterized cloud and convective precipitation.
- 6) Incorporation of the radiative property of cloud water and ice has a strong impact on the simulated temperature bias and radiation fields.

Comparing further with observed ISCCP cloudiness and cloud water and NCEP–DOE AMIP-II Reanalysis

relative humidity, we found that in all schemes examined in this study, cloudiness is controlled mainly by relative humidity, while the influence of cloud water is secondary. However, in observations, cloudiness is more strongly controlled by cloud water than by relative humidity. Our preliminary experiments to apply the direct relation between cloud water and cloudiness failed to improve the simulation, primarily due to poor skill in the simulation of cloud water. This strongly suggests that more work is needed to improve the cloud water parameterizations in current models, which might eventually improve the simulation of cloudiness.

Acknowledgments. We thank Drs. John Roads and Ming Ji for their support throughout the study. This study was supported by NSC 95-211-M133-001-AP4 and NOAA NA17RJ1231. The views expressed herein are those of the authors and do not necessarily reflect the views of NOAA. This work was also supported by the Korea Meteorological Administration Research and Development Program under Grant CATER 2007-4406 for S.-Y. Hong. We thank Ms. Diane Boomer for improving the readability of the paper. We also thank two anonymous reviewers for their helpful comments. The ISCCP, ERBE, and SRB datasets were obtained from the NASA Langley Research Center Atmospheric Science Data Center.

REFERENCES

- Adler, R. F., and Coauthors, 2003: The version-2 Global Precipitation Climatology Project (GPCP) Monthly Precipitation Analysis (1979–present). *J. Hydrometeorol.*, **4**, 1147–1167.
- Arakawa, A., and W. H. Schubert, 1974: Interaction of a cumulus cloud ensemble with the large-scale environment, Part I. *J. Atmos. Sci.*, **31**, 674–701.
- Bony, S., and K. A. Emanuel, 2001: A parameterization of the cloudiness associated with cumulus convection; evaluation using TOGA COARE data. *J. Atmos. Sci.*, **58**, 3158–3183.
- Boville, B. A., P. J. Rasch, J. J. Hack, and J. R. McCaa, 2006: Representation of clouds and precipitation processes in the Community Atmosphere Model version 3 (CAM3). *J. Climate*, **19**, 2184–2198.
- Bower, K. N., T. W. Choullarton, J. Latham, J. Nelson, M. B. Baker, and J. Jenson, 1994: A parameterization of warm clouds for use in atmospheric general circulation models. *J. Atmos. Sci.*, **51**, 2722–2732.
- Bretherton, C. S., J. R. McCaa, and H. Grenier, 2004a: A new parameterization for shallow cumulus convection and its application to marine subtropical cloud-topped boundary layers. Part I: Description and 1D results. *Mon. Wea. Rev.*, **132**, 864–882.
- , and Coauthors, 2004b: The EPIC 2001 stratocumulus study. *Bull. Amer. Meteor. Soc.*, **85**, 967–977.
- Chou, M.-D., 1992: A solar radiation model for use in climate studies. *J. Atmos. Sci.*, **49**, 762–772.

- , M. J. Suarez, C.-H. Ho, M. M.-H. Yan, and K.-T. Lee, 1998: Parameterizations for cloud overlapping and shortwave single-scattering properties for use in general circulation and cloud ensemble models. *J. Climate*, **11**, 202–214.
- , K.-T. Lee, S.-C. Tsay, and Q. Fu, 1999: Parameterization for cloud longwave scattering for use in atmospheric models. *J. Climate*, **12**, 159–169.
- Collins, W. D., and Coauthors, 2006: The formulation and atmospheric simulation of the Community Atmosphere Model version 3 (CAM3). *J. Climate*, **19**, 2144–2161.
- Covey, C., K. M. AchutaRao, U. Cubasch, P. Jones, S. J. Lambert, M. E. Mann, T. J. Phillips, and K. E. Taylor, 2003: An overview of results from the Coupled Model Intercomparison Project. *Global Planet. Change*, **37**, 103–133.
- Dai, A., 2006: Precipitation characteristics in eighteen coupled climate models. *J. Climate*, **19**, 4605–4630.
- Delworth, T. L., and Coauthors, 2006: GFDL's CM2 global coupled climate models. Part I: Formulation and simulation characteristics. *J. Climate*, **19**, 643–674.
- Dudhia, J., 1989: Numerical study of convection observed during the winter monsoon experiment using a mesoscale two-dimensional model. *J. Atmos. Sci.*, **46**, 3077–3107.
- Duynkerke, P. G., and J. Teixeira, 2001: Comparison of the ECMWF reanalysis with FIRE I observations: Diurnal variation of marine stratocumulus. *J. Climate*, **14**, 1466–1478.
- Ebert, E. E., and J. A. Curry, 1992: A parameterization of ice cloud optical properties for climate models. *J. Geophys. Res.*, **97**, 3831–3836.
- Ek, M. B., K. E. Mitchell, Y. Lin, E. Rogers, P. Grunmann, V. Koren, G. Gayno, and J. D. Tarpley, 2003: Implementation of Noah land surface model advances in the National Centers for Environmental Prediction operational mesoscale Eta model. *J. Geophys. Res.*, **108**, 8851, doi:10.1029/2002JD003296.
- Fowler, L. D., D. A. Randall, and S. A. Rutledge, 1996: Liquid and ice cloud microphysics in the CSU general circulation model. Part I: Model description and simulated microphysical processes. *J. Climate*, **9**, 489–529.
- Gettelman, A., E. J. Fetzer, A. Eldering, and F. W. Irion, 2006a: The global distribution of supersaturation in the upper troposphere from the atmospheric infrared sounder. *J. Climate*, **19**, 6089–6103.
- , W. D. Collins, E. J. Fetzer, A. Eldering, F. W. Irion, P. B. Duffy, and G. Bala, 2006b: Climatology of upper-tropospheric relative humidity from the atmospheric infrared sounder and implications for climate. *J. Climate*, **19**, 6104–6121.
- GFDL Global Atmospheric Model Development Team, 2004: The new GFDL global atmosphere and land model AM2–LM2: Evaluation with prescribed SST simulations. *J. Climate*, **17**, 4641–4673.
- Gordon, C., C. Cooper, C. A. Senior, H. Banks, J. M. Gregory, T. C. Johns, J. F. B. Mitchell, and R. A. Wood, 2000: The simulation of SST, sea ice extents and ocean heat transports in a version of the Hadley Centre coupled model without flux adjustments. *Climate Dyn.*, **16**, 147–168.
- Hong, S.-Y., and H.-L. Pan, 1996: Nonlocal boundary layer vertical diffusion in a medium-range forecast model. *Mon. Wea. Rev.*, **124**, 2322–2339.
- , H.-M. H. Juang, and Q. Zhao, 1998: Implementation of prognostic cloud scheme for a regional spectral model. *Mon. Wea. Rev.*, **126**, 2621–2639.
- , J. Dudhia, and S.-H. Chen, 2004: A revised approach to ice microphysical processes for the bulk parameterization of clouds and precipitation. *Mon. Wea. Rev.*, **132**, 103–120.
- Iacobellis, S. F., and R. C. J. Somerville, 2000: Implications of microphysics for cloud-radiation parameterizations: Lessons from TOGA COARE. *J. Atmos. Sci.*, **57**, 161–183.
- Kanamitsu, M., W. Ebisuzaki, J. Woollen, S.-K. Yang, J. J. Hnilo, M. Fiorino, and G. L. Potter, 2002a: NCEP–DOE AMIP-II Reanalysis (R-2). *Bull. Amer. Meteor. Soc.*, **83**, 1631–1643.
- , and Coauthors, 2002b: NCEP dynamical seasonal forecast system 2000. *Bull. Amer. Meteor. Soc.*, **83**, 1019–1037.
- Kärcher, B., and U. Lohmann, 2002: A parameterization of cirrus cloud formulation: Homogeneous freezing of supercooled aerosols. *J. Geophys. Res.*, **107**, 4010, doi:10.1029/2001JD000470.
- , J. Hendricks, and U. Lohmann, 2006: Physically based parameterization of cirrus cloud formation for use in global atmospheric models. *J. Geophys. Res.*, **111**, D01205, doi:10.1029/2005JD006219.
- Kessler, E., 1969: *On the Distribution and Continuity of Water Substance in Atmospheric Circulations*. Meteor. Monogr., No. 32, Amer. Meteor. Soc., 84 pp.
- Lin, Y.-L., R. D. Farley, and H. D. Orville, 1983: Bulk parameterization of the snow field in a cloud model. *J. Climate Appl. Meteor.*, **22**, 1065–1092.
- Lohmann, U., N. McFarlane, L. Levkov, K. Abdella, and F. Albers, 1999: Comparing different cloud schemes of a single column model by using mesoscale forcing and nudging technique. *J. Climate*, **12**, 438–461.
- Moorathi, S., and M. J. Suarez, 1992: Relaxed Arakawa–Schubert: A parameterization of moist convection for general circulation models. *Mon. Wea. Rev.*, **120**, 978–1002.
- Randall, D. A., 1995: Parameterizing fractional cloudiness produced by cumulus detrainment. *Proc. Workshop on Cloud Microphysics Parameterizations in Global Atmospheric Circulation Models*, Kananaskis, AB, Canada, WCRP-90, WMO/TD-713, 1–16.
- Reynolds, R. W., and T. M. Smith, 1994: Improved global sea surface temperature analyses using optimum interpolation. *J. Climate*, **7**, 929–948.
- Rossow, W. B., and R. A. Schiffer, 1999: Advances in understanding clouds from ISCCP. *Bull. Amer. Meteor. Soc.*, **80**, 2261–2287.
- Rotstain, L. D., B. F. Ryan, and J. J. Katzfey, 2000: A scheme for calculation of the liquid fraction in mixed-phase stratiform clouds in large-scale models. *Mon. Wea. Rev.*, **128**, 1070–1088.
- Rutledge, S. A., and P. V. Hobbs, 1983: The mesoscale and microscale structure and organization of clouds and precipitation in midlatitude cyclones. VIII: A model for the “seeder-feeder” process in warm-frontal rainbands. *J. Atmos. Sci.*, **40**, 1185–1206.
- Saito, K., and A. Baba, 1988: A statistical relation between relative humidity and the GMS observed cloud amount. *J. Meteor. Soc. Japan*, **66**, 187–192.
- Sardeshmukh, P. D., G. P. Compo, and C. Penland, 2000: Changes of probability associated with El Niño. *J. Climate*, **13**, 4268–4286.
- Senior, C. A., and J. F. B. Mitchell, 1993: Carbon dioxide and climate: The impact of cloud parameterization. *J. Climate*, **6**, 393–418.
- Slingo, A., 1989: A GCM parameterization for the shortwave radiation properties of water clouds. *J. Atmos. Sci.*, **46**, 1419–1427.
- , and J. M. Slingo, 1991: Response of the National Center for

- Atmospheric Research Community Climate Model to improvements in the representation of clouds. *J. Geophys. Res.*, **96**, 15 341–15 357.
- Slingo, J. M., 1987: The development and verification of a cloud prediction scheme for the ECMWF model. *Quart. J. Roy. Meteor. Soc.*, **113**, 899–927.
- Smith, R. N. B., 1990: A scheme for predicting layer clouds and their water content in a general circulation model. *Quart. J. Roy. Meteor. Soc.*, **116**, 435–460.
- Sommeria, G., and J. W. Deardorff, 1977: Subgrid-scale condensation in models of nonprecipitation clouds. *J. Atmos. Sci.*, **34**, 344–355.
- Stackhouse, P. W., Jr., and Coauthors, 2004: 12-year Surface Radiation Budget data set. *GEWEX News*, No. 14, International GEWEX Project Office, Silver Spring, MD, 10–12.
- Stephens, G. L., 2005: Cloud feedbacks in the climate system: A critical review. *J. Climate*, **18**, 237–273.
- Sundqvist, H., 1978: A parameterization scheme for non-convective condensation including prediction of cloud water content. *Quart. J. Roy. Meteor. Soc.*, **104**, 677–690.
- , E. Berge, and J. E. Kristjánsson, 1989: Condensation and cloud parameterization studies with a mesoscale numerical weather prediction model. *Mon. Wea. Rev.*, **117**, 1641–1657.
- Stevens, B., and Coauthors, 2001: Simulations of trade wind cumuli under a strong inversion. *J. Atmos. Sci.*, **58**, 1870–1891.
- , and Coauthors, 2005: Evaluation of large-eddy simulations via observations of nocturnal marine stratocumulus. *Mon. Wea. Rev.*, **133**, 1443–1462.
- Teixeira, J., 2001: Cloud fraction and relative humidity in a prognostic cloud fraction scheme. *Mon. Wea. Rev.*, **129**, 1750–1753.
- , and T. F. Hogan, 2002: Boundary layer clouds in a global atmospheric model: Simple cloud cover parameterizations. *J. Climate*, **15**, 1261–1276.
- Tiedtke, M., 1993: Representation of clouds in large-scale models. *Mon. Wea. Rev.*, **121**, 3040–3061.
- Tompkins, A. M., 2002: A prognostic parameterization for the subgrid-scale variability of water vapor and clouds in large-scale models and its use to diagnose cloud cover. *J. Atmos. Sci.*, **59**, 1917–1942.
- Weare, B. C., 2000: Near-global observations of low clouds. *J. Climate*, **13**, 1255–1268.
- , 2004: A comparison of AMIP II model cloud layer properties with ISCCP D2 estimates. *Climate Dyn.*, **22**, 281–291.
- Wyser, K., 1998: The effective radius in ice clouds. *J. Climate*, **11**, 1793–1802.
- Xu, K.-M., and D. A. Randall, 1996: A semiempirical cloudiness parameterization for use in climate models. *J. Atmos. Sci.*, **53**, 3084–3102.
- Zhao, Q., and F. H. Carr, 1997: A prognostic cloud scheme for operational NWP models. *Mon. Wea. Rev.*, **125**, 1931–1953.